

---

# Over-the-Air Beamforming with Reconfigurable Intelligent Surfaces

Zehra Yigit<sup>1,\*</sup>, Ertugrul Basar<sup>2</sup> and Ibrahim Altunbas<sup>1</sup>

<sup>1</sup>*Department of Electronics and Communication Engineering, Istanbul Technical University, Maslak 34469, Istanbul, Turkey.*

<sup>2</sup>*Communications Research and Innovation Laboratory (CoreLab), Department of Electrical and Electronics Engineering, Koç University, Sariyer 34450, Istanbul, Turkey.*

Correspondence\*:  
Zehra Yigit  
yigitz@itu.edu.tr

## ABSTRACT

Reconfigurable intelligent surface (RIS)-empowered communication is a revolutionary technology that enables to manipulate wireless propagation environment via smartly controllable low-cost reflecting surfaces. However, in order to outperform conventional communication systems, an RIS-aided system with solely passive reflection requires an extremely large surface. To meet this challenge, the concept of active RIS, which performs simultaneous amplification and reflection on the incident signal at the expense of additional power consumption, has been recently introduced. In this paper, deploying an active RIS, we propose a novel beamforming concept, *over-the-air beamforming*, for RIS-aided multi-user multiple-input single-output (MISO) transmission schemes without requiring any pre/post signal processing hardware designs at the transmitter and receiver sides. In the proposed over-the-air beamforming-based transmission scheme, the reflection coefficients of the active RIS elements are customized to maximize the sum-rate gain. To tackle this issue, first, a non-convex quadratically constrained quadratic programming (QCQP) problem is formulated. Then, using semidefinite relaxation (SDR) approach, this optimization problem is converted to a convex feasibility problem, which is efficiently solved using the CVX optimization toolbox. Moreover, taking inspiration from this beamforming technique, a novel high-rate receive index modulation (IM) scheme with a low-complexity sub-optimal detector is developed. Through comprehensive simulation results, the sum-rate and bit error rate (BER) performance of the proposed designs are investigated.

**Keywords:** Reconfigurable intelligent surface (RIS), active RIS, over-the-air beamforming, multi-user (MU) transmission, index modulation (IM).

## 1 INTRODUCTION

Customizing propagation environment via reconfigurable intelligent surfaces (RISs) has been an appealing field for wireless communication and provides novel insights about future generation networks. These light-weight and cost-effective electronic elements have been regarded as a game changer technology for conventional communication systems with power-hungry and complex hardware designs (Basar et al., 2019). Particularly, RISs are programmable metasurfaces that are capable of configuring the propagation environment in a desired manner via performing reflection, amplification, absorption, refraction, etc. (Di Renzo et al., 2020). However, the most of the extant literature particularly focuses on the application

of the RIS with passive reflection in various emerging systems (Basar et al., 2019; Di Renzo et al., 2020; Gong et al., 2020).

In the early studies, a passive RIS is deployed for enhancing transmit signal quality of single-antenna (Basar, 2019) and multiple-antenna systems (Yu et al., 2019; Zhang et al., 2020; Yigit et al., 2020). In subsequent studies, an RIS is facilitated for numerous objectives of single-user and multi-user systems, such as promoting energy-efficiency (Huang et al., 2019; Björnson et al., 2019), enhancing error performance (Ye et al., 2020; Ferreira et al., 2020) and improving achievable rate (Zhang and Zhang, 2020; Perović et al., 2021; Di et al., 2020). Further, novel deep learning-based solutions for passive RIS designs (Taha et al., 2021; Kundu and McKay, 2021) and security enhanced RIS-aided communication systems (Almohamad et al., 2020; Dong and Wang, 2020) are proposed. On the other hand, index modulation (IM) principle, which is emerged as a promising energy-efficient solution to meet high data-rate demand of future wireless networks (Basar et al., 2017), is beneficially amalgamated into the RIS-empowered communication (Basar, 2020; Li et al., 2021). Considering more conventional IM designs, (Li et al., 2021; Basar, 2020) put forward RIS-aided receive IM schemes, which maximize the signal powers of the target receive antennas. However, in (Guo et al., 2020; Lin et al., 2020), novel reflection modulation (RM) concepts, which innovatively utilize the RISs for delivering additional information, are proposed. Above all, main limitation of the aforementioned studies is the lack of comprehensive practical insights on considered system configurations. Towards this aim, different RIS prototypes are introduced for real-time implementations in (Dai et al., 2020; Tang et al., 2020), and realistic physical channel models for millimeter-wave (mmWave) (Basar et al., 2021) and sub-6 GHz bands (Kilinc et al., 2021; Yigit et al., 2021a) are presented. Nevertheless, the abovementioned system designs suffer from the multiplicative path attenuation due to the inherent drawback of the RIS-aided designs, and achieve negligible performance gains over the conventional communication systems.

Recently, to tackle above challenges, the concept of active RIS, which performs simultaneous amplification and reflection on the incident wave, is introduced in (Zhang et al., 2021; Long et al., 2021). Accordingly, the magnitudes and the phases of the reflecting elements of the active RIS, which are equipped with additional power amplifiers, are properly tuned in a customized way (Basar and Poor, 2021). Therefore, at the cost of additional power consumption, active RIS-aided systems are capable of achieving enhanced capacity gains (Long et al., 2021). In a recent study on designing active RISs, a dynamic and fixed hybrid RIS architectures are constructed via leveraging power amplifiers and radio frequency (RF) chains as active elements (Nguyen et al., 2022). Further, for improving the data rate, a new RM design, which employs the sub-groups of a hybrid RIS as information transfer units, is presented in (Yigit et al., 2021b). In follow-up studies, the concept of the active RIS is deployed for beamforming optimization of the RIS-aided multi-user systems (Gao et al., 2022; Thanh Nguyen et al., 2022). Above all, the potential of the active RIS-aided systems for achieving enormous performance gains will enable to develop promising solutions for future research.

In this study, unlike the conventional precoding techniques that employ power-hungry and hardware-complex devices (Sohrabi and Yu, 2016), for RIS-aided multi-user downlink transmission systems, we propose a novel *over-the-air beamforming* technique with the aid of an active RIS to exploit its capability of manipulating the magnitude of the incident wave. In other words, the main motivation of the over-the-air beamforming scheme is to simplify the transmitter and receiver ends of the overall network while transferring inter-user interference elimination tasks completely to an active RIS. In the proposed over-the-air beamforming-based transmission scheme, it is assumed that a multiple-antenna transmitter serves  $K$  single-antenna users through an active RIS without utilizing any other signal processing tasks at the

transmitter and the receiver sides. Then, the reflection coefficients of the active RIS is properly adjusted to maximize the sum-rate of the overall system. To address this issue, a non-convex quadratically constrained quadratic programming (QCQP) problem is formulated. However, since it is challenging to solve, exploiting a semidefinite relaxation (SDR) approach, the problem is converted to a convex feasibility problem that can be solved via CVX optimization toolbox. Moreover, the concept of over-the-air beamforming is adopted to propose a novel active RIS-aided receive IM system for single-user multi-antenna uplink transmission. Contrary to the traditional receive IM systems (Luo et al., 2021; Zhang et al., 2013), in the proposed system, since no precoding is applied at the transmitter, the reflection coefficients of the active RIS are rectified to steer the incident signal into the intended receive antenna. On the other hand, since the receive IM scheme benefits from the multi-antenna transmission at the user side and IM system design at the receiver side, it shows the favourable features of both, such as high spectral efficiency and improved performance. Furthermore, the sum-rate and bit error rate (BER) performance of the proposed over-the-air beamforming-based transmission schemes are investigated through extensive computer simulations.

The rest of the paper is organized as follows. In Section II, after giving a short review of the conventional zero forcing (ZF) precoding, we introduce the system model of the proposed over-the-air beamforming-based multi-user multi-antenna transmission scheme. In Section III, the over-the-air beamforming-based receive IM scheme and its low-complexity receiver detection are introduced. Section III provides the sum-rate and BER results of the proposed over-the-air beamforming based transmission systems, and the conclusions are drawn in Section IV.

*Notations:* Throughout this paper, matrices and vectors are denoted by boldface upper-case and boldface lower-case letters, respectively.  $(\cdot)^T$  represents transpose and  $(\cdot)^H$  denotes the Hermitian transpose operation.  $\|\cdot\|$ ,  $\text{rank}(\cdot)$ ,  $\text{Tr}(\cdot)$  and  $\text{diag}(\cdot)$  are stand for rank, trace and diagonalization of a matrix, respectively. Absolute value of a scalar is denoted by  $|\cdot|$ , while  $\circ$  represents the Hadamard product.  $\mathbb{E}\{\cdot\}$  is used for expectation and  $\mathcal{CN}(\mu, \sigma^2)$  represents a complex Gaussian random variable with  $\mu$  mean and  $\sigma^2$  variance.  $\mathbf{I}$  stands for the identity matrix, while  $\mathcal{O}(\cdot)$  denotes big  $\mathcal{O}$  notation.

## 2 OVER-THE-AIR BEAMFORMING WITH RIS

In this section, after a review of conventional transmit precoding, the over-the-air beamforming concept is introduced for multi-user multiple-input single-output (MISO) downlink transmission systems.

### 2.1 Conventional Transmit Precoding

Considering a typical multi-user downlink transmission system without an RIS, where a base station (BS) transmitter (T) with  $T_x$  antennas is assumed to perform ZF precoding to alleviate interference between  $K$  single-antenna users (Spencer et al., 2004). Let  $\mathbf{F} \in \mathbb{C}^{K \times T_x} = \sqrt{L_D} \bar{\mathbf{F}}$  represents the channel matrix of the direct links between the T and the users, where  $\bar{\mathbf{F}} \in \mathbb{C}^{K \times T_x}$  is modeled as independent Rayleigh fading channel matrix with  $\sim \mathcal{CN}(\mathbf{0}, \mathbf{I})$  and  $L_D$  is the corresponding path attenuation, which is calculated as  $L_D = C_0 d_D^{-\beta_D}$ , where  $C_0$  is the reference path attenuation at a distance of 1 meter (m) and  $d_D$  is the distance between T and the users. Then, in the case of each transmit antenna is assigned to a different user, i.e.,  $T_x = K$ , the received signal of the  $k$ -th user ( $U_k$ ), for  $k \in \{1, 2, \dots, K\}$ , becomes

$$y_k = \mathbf{f}_k \mathbf{w}_k^H x_k + \sum_{i \neq k}^K \mathbf{f}_k \mathbf{w}_i^H x_i + c_k \quad (1)$$

where  $x_k$  being an  $M$ -ary phase shift keying (PSK) signal to be transmitted over the  $k$ -th transmit antenna. Here,  $\mathbf{f}_k \in \mathbb{C}^{1 \times T_x}$  is the  $k$ -th row of the channel matrix  $\mathbf{F}$  corresponding to the channel vector between T- $U_k$ ,  $\mathbf{w}_k \in \mathbb{C}^{1 \times T_x}$  is the precoding vector for  $U_k$  and  $c_k \sim \mathcal{CN}(0, \sigma_s^2)$  is the static noise at  $U_k$ . Therefore, the signal-to-interference-plus-noise-ratio (SINR) at  $U_k$  can be calculated as

$$\gamma_k = \frac{\|\mathbf{f}_k \mathbf{w}_k^H\|^2}{\sum_{i \neq k}^K \|\mathbf{f}_k \mathbf{w}_i^H\|^2 + \sigma_s^2}. \quad (2)$$

Moreover, the overall transmit ZF precoding matrix, exploiting the perfect CSI, can be obtained as (Spencer et al., 2004)

$$\mathbf{W} = \sqrt{\zeta} (\mathbf{F}^H \mathbf{F})^{-1} \mathbf{F}^H. \quad (3)$$

where  $\mathbf{W} \in \mathbb{C}^{T_x \times K} = [\mathbf{w}_1^H, \dots, \mathbf{w}_K^H]$  and  $\zeta$  is a scaling constant to meet the transmit power constraint  $P_{BS}$ , such that  $\mathbb{E} \{ \mathbf{W} \mathbf{W}^H \} = P_{BS}$ .

## 2.2 System Model of Over-the-Air Beamforming with RIS

In this subsection, the system model of the over-the-air beamforming-based multi-user transmission system is introduced.

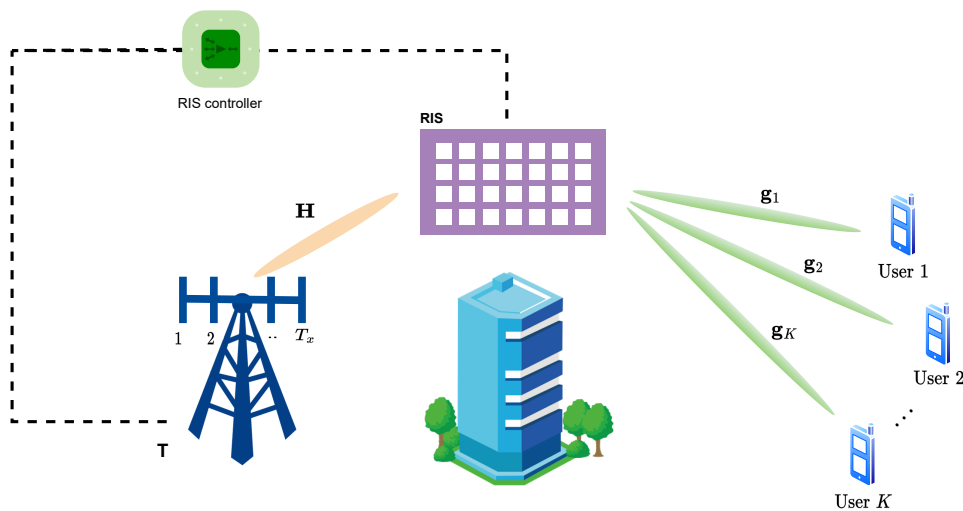


**Figure 1.** Over-the-air beamforming-based multi-user downlink transmission system.

An overwhelming literature on passive RIS-aided multi-user transmission deploys the RIS as a passive beamformer, after a preprocessing is conducted at the transmitter (Wu and Zhang, 2019; Yan et al., 2020). However, in the proposed over-the-air beamforming concept, contrary to this traditional perspective, both the active and the passive beamforming are carried out only at the RIS with active reflecting elements.

As given in Fig. 1, in the proposed scheme, the direct transmission links between T with  $T_x$  antennas and  $K$  single-antenna users are neglected due to obstacles, thus, the communication is established through an active RIS with  $N$  reflecting elements. In the proposed over-the-air beamforming-based multi-user transmission, it is assumed that T and the users have the perfect channel state information (CSI) about

T-RIS and RIS-users channels, which is conveyed to a smart RIS controller via a feedback control link (Wu and Zhang, 2019). Moreover, in the proposed system, it is assumed that each transmit antenna is dedicated to a different user, that is,  $T_x = K$  number of transmit antennas with  $M$ -PSK are employed, and a spectral efficiency of  $\eta_{\text{MU}} = T_x \log_2(M)$  [bits/s/Hz] is achieved. Then, at the transmitter side, without requiring any additional signal processing approaches for interference mitigation, the overall signal is conveyed to the users through the RIS. Towards this aim, the RIS elements are assumed to be equipped with additional power circuitry to modify both the magnitude and the phase of the incident signal (Zhang et al., 2021; Nguyen et al., 2022; Yigit et al., 2021b). Hence, unlike the traditional beamforming techniques that employ complex and power-hungry signal processing hardware (Sohrabi and Yu, 2016; El Ayach et al., 2014), the RIS is designed as a beamformer to alleviate multi-user interference by adjusting the amplitude and phase of each reflecting element.

Let us assume that the channels between T-RIS are presented by the matrix  $\mathbf{H} \in \mathbb{C}^{N \times T_x} = \sqrt{L_T} \bar{\mathbf{H}}$  and  $\mathbf{g}_k \in \mathbb{C}^{1 \times N} = \sqrt{L_k} \bar{\mathbf{g}}_k$  represents the vector of channel coefficients between the RIS and  $\mathbf{U}_k$ , where  $L_T$  and  $L_k$  correspond to path attenuation between T-RIS and RIS- $\mathbf{U}_k$  links for  $k \in \{1, 2, \dots, K\}$ , respectively. Here, for  $d_T$  and  $d_k$  being the corresponding distances, using a well-known distance-dependent model, the path attenuations are obtained as  $L_T = C_0 d_T^{-\beta_T}$  and  $L_k = C_0 d_k^{-\beta_k}$ , where  $\beta_T$  and  $\beta_k$  are the path loss exponents at T-RIS and RIS- $\mathbf{U}_k$ , respectively. In the proposed system, the matrix  $\bar{\mathbf{H}} \in \mathbb{C}^{N \times K}$  and the vector  $\bar{\mathbf{g}}_k \in \mathbb{C}^{1 \times N}$  are both modeled as Rayleigh fading channels, whose each element is an independent and identically distributed (i.i.d.) Gaussian random variable with  $\sim \mathcal{CN}(0, 1)$ . In addition, the RIS architecture that is equipped with additional power circuitry to operate as an active RIS (Zhang et al., 2021), is represented in a diagonal matrix  $\Psi \in \mathbb{C}^{N \times N} = \text{diag}\{\alpha_1 e^{j\phi_1}, \alpha_2 e^{j\phi_2}, \dots, \alpha_N e^{j\phi_N}\}$ , where  $\alpha_n > 1$  and  $\phi_n \in [-\pi, \pi]$  being the amplitude and phase of the  $n$ -th reflecting element for  $n \in \{1, 2, \dots, N\}$ . Therefore, for the overall transmit signal being  $\mathbf{x} \in \mathbb{C}^{T_x \times 1} = [x_1, x_2, \dots, x_K]^T$ , the received signal at  $\mathbf{U}_k$  is obtained as

$$y_k = \sqrt{P_k} \mathbf{g}_k \Psi \mathbf{H} \mathbf{x} + \mathbf{g}_k \Psi \mathbf{v}^T + n_k \quad (4)$$

where  $\mathbb{E}\{\mathbf{x}^H \mathbf{x}\} = 1$ . Here,  $P_k$  is the power introduced by the  $k$ -th transmit antenna, the vector  $\mathbf{v} \in \mathbb{C}^{1 \times N}$  represents the thermal noise generated from power amplifier circuits of active reflecting elements (Zhang et al., 2021) and  $n_k$  is the static noise term at  $\mathbf{U}_k$ , where  $\mathbf{v} \sim \mathcal{CN}(\mathbf{0}, \mathbf{I}_N \sigma_v^2)$  and  $n_k \sim \mathcal{CN}(0, \sigma_s^2)$  for  $\sigma_v^2$  and  $\sigma_s^2$  being the corresponding noise variances of dynamic and static noise figures, respectively. Moreover, at the user side, since the received superposed signal at  $\mathbf{U}_k$  (4) includes the targeted and interference signals, it can be rewritten as

$$y_k = \sqrt{P_k} \mathbf{g}_k \Psi \mathbf{h}_k x_k + \sqrt{P_k} \sum_{i \neq k}^K \mathbf{g}_k \Psi \mathbf{h}_i x_i + \mathbf{g}_k \Psi \mathbf{v}^T + n_k \quad (5)$$

where  $\mathbf{h}_k \in \mathbb{C}^{N \times 1}$  is the  $k$ -th column of the channel matrix  $\mathbf{H}$  corresponding to the channel vector between the  $k$ -th transmit antenna and the RIS. At this point, the SINR at  $\mathbf{U}_k$  can be calculated as:

$$\gamma_k = \frac{P_k \|\mathbf{g}_k \Psi \mathbf{h}_k\|^2}{P_k \sum_{i \neq k}^K \|\mathbf{g}_k \Psi \mathbf{h}_i\|^2 + \|\mathbf{g}_k \Psi \mathbf{v}^T\|^2 + \sigma_s^2}. \quad (6)$$

Accordingly, the sum-rate of the overall system becomes:

$$R = \sum_{k=1}^K \log_2(1 + \gamma_k). \quad (7)$$

Then, to maximize this sum-rate, the reflection coefficients of the active RIS elements are optimized. In what follows, the corresponding problem formulation and the proposed solution are presented.

### 2.3 Problem Formulation and Proposed Solution

In the over-the-air beamforming-based multi-user transmission scheme, interference cancellation is performed at the RIS without employing any additional integrated high-cost signal processing circuitry, such as multiple RF chains, either at T or user sides. For this purpose, the reflection coefficients of the RIS are adjusted to maximize the SINR of the intended  $U_k$ . Therefore, to deal with this problem, the following QCQP problem is formulated

$$(P1) : \max_{\Psi} \gamma_k \quad (8)$$

$$\text{s.t. } P_k \|\mathbf{g}_k \Psi \mathbf{h}_k\|^2 \geq \Gamma_k \left( P_k \sum_{i \neq k} \|\mathbf{g}_k \Psi \mathbf{h}_i\|^2 + \|\mathbf{g}_k \Psi \mathbf{v}^T\|^2 + \sigma_s^2 \right) \quad (9)$$

$$P_{BS} \|\Psi \mathbf{H}\|^2 + \|\Psi\|^2 \sigma_s^2 \leq P_A \quad (10)$$

where  $\Gamma_k$  is the minimum SINR requirement of  $U_k$ ,  $P_{BS} = KP_k$ , and  $P_A$  is the maximum reflection power introduced by the active reflecting elements. Please note that for the over-the-air beamforming-based multi-user systems, the total power  $P_T$  is the sum of power dissipated at the transmitter ( $P_{BS}$ ) and the RIS ( $P_A$ ), that is  $P_T = P_A + P_{BS}$ , while for the conventional transmission without RIS  $P_T = P_{BS}$ .

Then, using the Cauchy-Schwarz inequality, the constraint in (10) can be rewritten as

$$\|\Psi\|^2 \leq \frac{P_A}{P_{BS} \|\mathbf{H}\|^2 + \sigma_s^2}. \quad (11)$$

Therefore, since the problem (P1) is non-convex and it is difficult to obtain an optimal solution, we resort to the SDR technique and define new variables  $\mathbf{A}_k \in \mathbb{C}^{N \times N} = \mathbf{h}_k^H \mathbf{h}_k$ ,  $\mathbf{B}_k \in \mathbb{C}^{N \times N} = \mathbf{g}_k^H \mathbf{g}_k$  and  $\mathbf{V} = \mathbf{v} \mathbf{v}^H$ . In light of these, the SINR of the  $k$ -th user in (6) can be rewritten as

$$\gamma_k = \frac{P_k \text{Tr}(\mathbf{Q}_k \mathbf{Z})}{\sum_{i \neq k} P_i \text{Tr}(\mathbf{Q}_i \mathbf{Z}) + \text{Tr}(\mathbf{Q}_m \mathbf{Z}) + \sigma_s^2} \geq \Gamma_k \quad (12)$$

where  $\mathbf{Q}_k \in \mathbb{C}^{N \times N} = \mathbf{A}_k \circ \mathbf{B}_k$ ,  $\mathbf{Q}_i \in \mathbb{C}^{N \times N} = \mathbf{A}_i \circ \mathbf{B}_k$  and  $\mathbf{Q}_m \in \mathbb{C}^{N \times N} = \mathbf{V}_k \circ \mathbf{B}_k$ , while  $\mathbf{Z} \in \mathbb{C}^{N \times N} = \mathbf{z} \mathbf{z}^H$  for  $\mathbf{z} \in \mathbb{C}^{N \times 1}$  being a vector consisting the non-zero diagonal elements of the reflection matrix  $\Psi$ , i.e.,  $\mathbf{z} = [\alpha_1 e^{j\phi_1}, \alpha_2 e^{j\phi_2}, \dots, \alpha_N e^{j\phi_N}]^H$  (Zhang, 2017; Ye et al., 2020). Therefore, the maximization problem (P1) is equivalently defined as

$$(P2) : \max_{\mathbf{z}} \gamma_k \quad (13)$$

$$\text{s.t. } P_k \text{Tr}(\mathbf{Q}_k \mathbf{Z}) - \Gamma_k \left( \sum_{i \neq k} P_k \text{Tr}(\mathbf{Q}_i \mathbf{Z}) + \text{Tr}(\mathbf{Q}_m \mathbf{Z}) + \sigma_s^2 \right) \geq 0 \quad (14)$$

$$\text{Tr}(\mathbf{Z}) \leq \frac{P_A}{P_{\text{BS}} \text{Tr}(\mathbf{H}\mathbf{H}^H) + \sigma_s^2}. \quad (15)$$

Here,  $\mathbf{Z}$  is a positive semidefinite matrix and  $\text{rank}(\mathbf{Z}) = 1$ . However, since the rank-one constraint is non-convex, we remove this constraint and reformulate (P2) as a convex feasibility problem as follows

$$(P3) : \text{Find } \mathbf{Z} \quad (16)$$

$$\text{s.t. } P_k \text{Tr}(\mathbf{Q}_k \mathbf{Z}) - \Gamma_k \left( \sum_{i \neq k} P_k \text{Tr}(\mathbf{Q}_i \mathbf{Z}) + \text{Tr}(\mathbf{Q}_m \mathbf{Z}) + \sigma_s^2 \right) \geq 0 \quad (17)$$

$$\text{Tr}(\mathbf{Z}) \leq \frac{P_A}{P_{\text{BS}} \text{Tr}(\mathbf{H}\mathbf{H}^H) + \sigma_s^2}. \quad (18)$$

Finally, through the existing solvers of CVX toolbox (Grant and Boyd, 2008), a feasible solution of (P3) satisfying the inequality constraints in (17) and (18) is obtained. However, after the relaxation, the optimal solution of (P3) cannot always ensure the rank-one solution. Therefore, for  $\tilde{\mathbf{Z}}$  being the optimal solution of the problem (P3), using the eigenvalue decomposition of  $\tilde{\mathbf{Z}} = \mathbf{U}\mathbf{\Sigma}\mathbf{U}^H$ , the estimated  $\mathbf{z}$  is sub-optimally obtained as

$$\tilde{\mathbf{z}} = \mathbf{U}\mathbf{\Sigma}^{1/2}\mathbf{r}^H \quad (19)$$

where  $\mathbf{r} \in \mathbb{C}^{1 \times N}$  is a Gaussian random vector with  $\sim \mathcal{CN}(\mathbf{0}, \mathbf{I})$ , where  $\mathbf{U} \in \mathbb{C}^{N \times N}$  is a unitary matrix of eigenvectors and  $\mathbf{\Sigma} \in \mathbb{C}^{N \times N}$  is a diagonal matrix of eigenvalues. Then, after determining optimized reflection matrix, the RIS performs over-the-air beamforming in order to alleviate the user interference.

### 3 OVER-THE-AIR RECEIVE INDEX MODULATION

In this section, the proposed over-the-air beamforming concept is adopted to a novel receive IM transmission scheme. Considering the over-the-air beamforming approach given in Section II, a single-user uplink transmission of an active RIS-aided IM transmission system is developed.

#### 3.1 System Model of Over-the-Air Receive IM

As given in Fig. 2, in the proposed IM system, due to presence of the obstacles over the direct links, a multi-antenna user communicates with an  $R_x$ -antenna receiver (R) through an RIS with  $N$  reflecting elements. Besides, an RIS controller is attached to the RIS that exchanges the information through a feedback control link. In the proposed system, considering the IM transmission principle (Basar, 2020), an over-the-air receive IM scheme is developed. Unlike traditional receive IM schemes (Stavridis et al., 2012; Zhang et al., 2013; Luo et al., 2021) that deploy transmit precoding techniques via high-cost hardware devices for preprocessing the transmit signal before its transmission, the proposed receive IM scheme employs the RIS as a signal processing unit and apply an over-the-air beamforming at the RIS. In the over-the-air receive IM scheme, at the user side, the conventional multi-antenna transmission is considered. Moreover, in order to attain higher data rates, extra information bits are conveyed via indicating the active

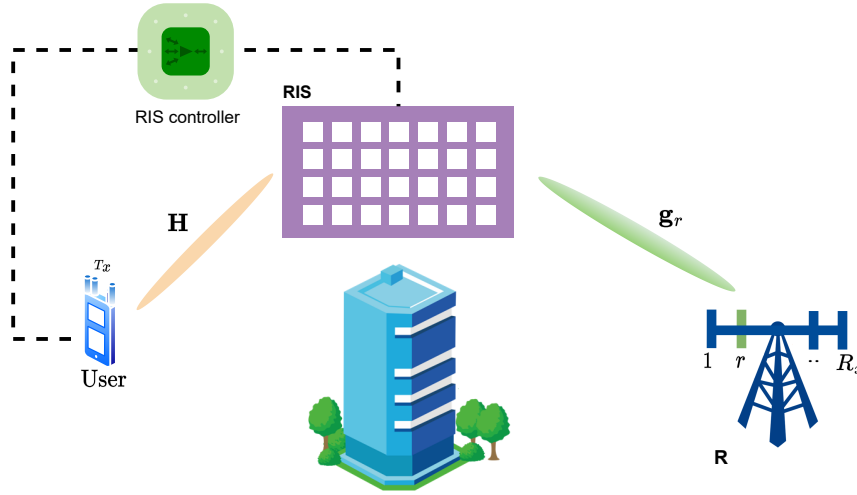


**Figure 2.** Over-the-air receive IM scheme.

receive antenna index. Therefore, the incoming information bits are used to determine the modulated  $M$ -PSK symbols for each of the available  $T_x$  transmit antennas, as well as to specify the active receive antenna index, one out of  $R_x$  receive antennas. Therefore, the spectral efficiency achieved by this novel receive IM scheme is calculated as

$$\eta_{\text{IM}} = T_x \log_2(M) + \log_2(R_x) \quad [\text{bits/s/Hz}]. \quad (20)$$

In this system, the information of the active receive antenna index and perfect channel knowledge of user-RIS and RIS-R links is shared by the user to the RIS through the smart controller. Then, the reflection coefficient of the RIS elements are adjusted to ensure that the target receive antenna has the strongest received signal power. In other words, by the means of active reflecting elements, the RIS acts as a kind of digital beamformer and steers the overall signal along the desired receive antenna direction.

Let the multi-path fading channels between user-RIS and RIS-R links are modeled as the independent Rayleigh fading channels, which are denoted by the channel matrices of  $\mathbf{H} \in \mathbb{C}^{N \times T_x}$  and  $\mathbf{G} \in \mathbb{C}^{R_x \times N} = [\mathbf{g}_1^T, \mathbf{g}_2^T, \dots, \mathbf{g}_{R_x}^T]^T$ , respectively, where  $\mathbf{g}_r \in \mathbb{C}^{1 \times N}$  is the  $r$ -th row of the the channel matrix  $\mathbf{G}$  corresponding to the channel vector between the RIS and the  $r$ -th receive antenna for  $r \in \{1, 2, \dots, R_x\}$ . Therefore, for  $x_t$  being the  $M$ -PSK modulated signal transmitted from the  $t$ -th transmit antenna, the overall transmit signal becomes  $\mathbf{x} \in \mathbb{C}^{T_x \times 1} = [x_1, \dots, x_{T_x}]^T$ , where  $\mathbb{E}\{\mathbf{x}^H \mathbf{x}\} = 1$  and  $t \in \{1, 2, \dots, T_x\}$ . Then, the received signal at the target receive antenna  $r$  is obtained as

$$y_r = \sqrt{P_{\text{BS}}} \mathbf{g}_r \Psi_r \mathbf{H} \mathbf{x} + \mathbf{g}_r \Psi_r \mathbf{v} + n_r \quad (21)$$

where  $\Psi_r \in \mathbb{C}^{N \times N}$  is the optimized diagonal reflection matrix for the corresponding  $r$ -th receive antenna. It is worth noting that according to incoming spatial bits, if the  $r$ -th receive antenna is activated, it is ensured that the signal power of the  $r$ -th received antenna is much stronger than the others:

$$\|\mathbf{g}_r \Psi_r \mathbf{H}\|^2 \gg \sum_{i \neq r} \|\mathbf{g}_i \Psi_r \mathbf{H}\|^2. \quad (22)$$



Therefore, to address this problem, for  $\Theta_r = \text{diag}(\mathbf{g}_r)\mathbf{H}$  and  $\mathbf{z} \in \mathbb{C}^{1 \times T_x} = \text{diag}(\Psi_r)$ , a QCQP optimization problem is formulated as

$$(P4) : \max_{\Psi} \mathbf{z}^H \Theta_r \Theta_r^H \mathbf{z} \quad (23)$$

$$\text{s.t. } P_{\text{BS}} \|\Psi_r \mathbf{H}\|^2 + \|\Psi_r\|^2 \sigma_s^2 \leq P_A. \quad (24)$$

Then, resorting to SDR, the problem (P4) is expressed as

$$(P5) : \max_{\mathbf{Z}} \text{Tr}(\Delta_r \mathbf{Z}) \quad (25)$$

$$\text{s.t. } \text{Tr}(\Delta_r \mathbf{Z}) - \delta_r \sum_{i \neq r}^{R_x} \text{Tr}(\Delta_i \mathbf{Z}) \geq 0 \quad (26)$$

$$\text{Tr}(\mathbf{Z}) \leq \frac{P_A}{P_{\text{BS}} \text{Tr}(\mathbf{H}\mathbf{H}^H) + \sigma_s^2}. \quad (27)$$

Here, for  $\delta_r \gg 1$ ,  $\Delta_r \in \mathbb{C}^{N \times N} = \Theta_r \Theta_r^H$  and  $\mathbf{Z} = \mathbf{z}\mathbf{z}^H$ , the problem (P5) is solved using CVX solvers (Grant and Boyd, 2008). Then, following the same processes as in the multi-user downlink transmission in Section II, the sub-optimal estimate of  $\mathbf{z}$ , is obtained as given in (19). Then, the resulting RIS reflection matrix enables that the overall signal is oriented in the direction of the target receive antenna.

### 3.2 Low-Complexity Successive Greedy Detector

In the subsection that follows, a sub-optimal successive detection algorithm for the proposed receive IM scheme is proposed. In the proposed system, after the optimization of the reflection matrix  $\Psi_r$  for the specified  $r$ -th receive antenna, it is straightforward to exploit a maximum likelihood (ML) detector that jointly estimates the "spatial symbol"  $r$  and the overall transmit signal vector  $\mathbf{x}$  as follows

$$[\hat{r}, \hat{\mathbf{x}}] = \arg \min_{r, \mathbf{x}} \sum_{j=1}^{R_x} \left| y_j - \sqrt{P_{\text{BS}}} \mathbf{g}_j \Psi_r \mathbf{H} \mathbf{x} \right|^2. \quad (28)$$

However, in the proposed receive IM scheme, in order to save the computational complexity, instead of considering joint detection, the receiver reconstructs the transmit information via a low-complexity greedy detector that perform the successive detection in the following way. First, using amplitude detectors, the index of the active receive antenna is detected as

$$\hat{r} = \arg \max_{j \in \{1, \dots, R_x\}} |y_j|. \quad (29)$$

Then, exploiting the maximum likelihood (ML) detector, the transmit signal vector  $\mathbf{x}$  is estimated, by considering all possible  $\mathbf{x}$  realizations, as follows

$$\hat{\mathbf{x}} = \arg \min_{\mathbf{x}} \left| y_{\hat{r}} - \sqrt{P_{\text{BS}}} \mathbf{g}_{\hat{r}} \Psi_r \mathbf{H} \mathbf{x} \right|^2. \quad (30)$$

Moreover, from the computational complexity standpoint, we note that since the complexity of SDR problem (P5) is  $\mathcal{O}(N^{4.5})$  (Luo et al., 2010), the overall complexity of the greedy detector approximates

to  $\sim \mathcal{O}(M^{T_x} + T_x)$ , while the complexity for the joint ML detector is  $\sim \mathcal{O}((M^{T_x} + T_x + N^{4.5})R_x^2)$ , which grows exponentially with increasing  $N$  and  $R_x$ . Therefore, comparing to the joint ML detection, the proposed greedy detector offers a significant reduction in computational burden.

## 4 NUMERICAL RESULTS

In this section, the sum-rate and BER performance of the proposed over-the-air beamforming-based multi-user multi-antenna downlink transmission and uplink receive IM schemes are presented through the Monte Carlo simulations. Moreover, comparing to the ZF-based conventional transmission schemes (Zhang et al., 2013), the improved performance of the over-the-air beamforming-based systems are illustrated.

In all computer simulations, the following system setups are considered: the reference path loss value is  $C_0 = -30$  dBm, the noise variances are  $\sigma_v^2 = \sigma_s^2 = -90$  dBm, the path loss exponents for the RIS-aided systems are  $\beta_T = 2.2$  and  $\beta_k = 2.8$  and for the conventional direct transmission, it is  $\beta_D = 3.5$  (Nguyen et al., 2022), the distances are  $d_T = 20$ ,  $d_R = 30$  m and  $d_D = 50$  m.

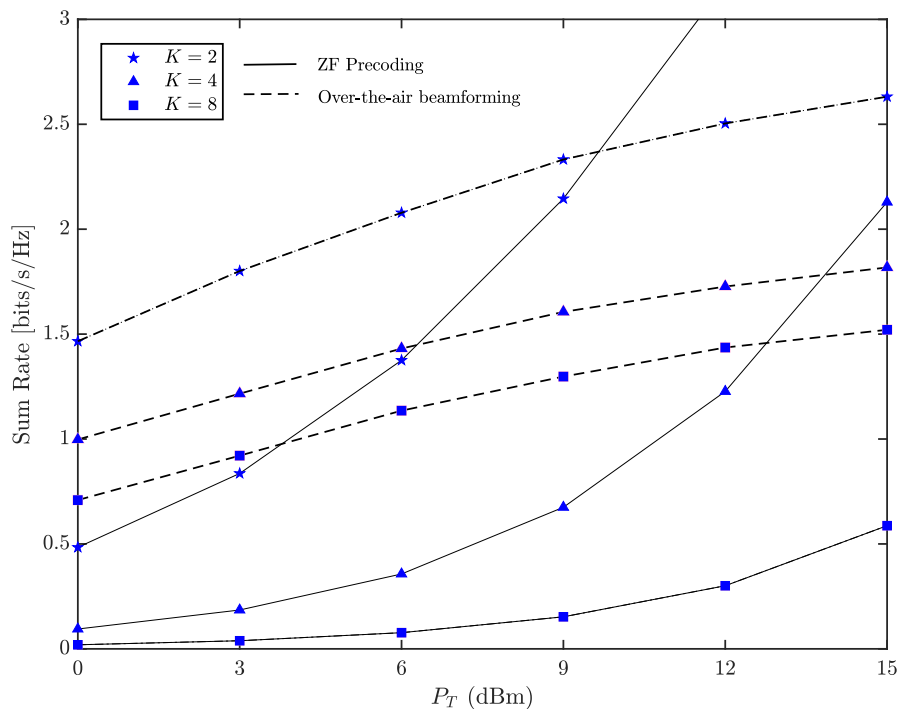


**Figure 3.** Sum-rate comparison of the proposed over-the-air beamforming and the classical transmit ZF precoding for  $K \in \{2, 4, 8\}$ .

### 4.1 Multi-user downlink transmission

In this subsection, the sum-rate results of an active RIS-aided multi-user downlink system with the proposed over-the-air-beamforming is demonstrated.

In Figure 3, the sum rate of the downlink multi-antenna transmission scheme based on the conventional transmit ZF precoding (Spencer et al., 2004) and the novel over-the-air beamforming has been carried out for  $K \in \{2, 4, 8\}$  and quadrature PSK (QPSK), i.e.,  $M = 4$ . Here, for the over-the-air beamforming with

$N = 16$ , the transmitter power is assumed to be  $P_{BS} = 0$  dBm, while, for a fair comparison, the transmit power of the conventional ZF precoder is equated to the total power  $P_T$ , where  $P_T = P_{BS} + P_A$  for the RIS-aided system. Comparing these two schemes, it is obvious that at lower  $P_T$  values, the over-the-air beamforming based multi-user transmission scheme attains higher sum-rate than the classical transmit ZF precoding technique (Spencer et al., 2004). However, for  $K = 2$  and  $K = 4$ , as  $P_T$  increases, the performance of ZF gradually begins to exceed the performance of the proposed beamforming scheme. Nevertheless, for  $K = 4$ , the ZF precoder achieves only a slight gain over the proposed beamforming concept at  $P_T = 15$  dBm. It can be also deduced from Figure 3 that an increase in the total number of users rapidly decreases ZF sum-rate, however, such a severe performance loss is not observed in the proposed over-the-air beamforming-based system. Moreover, when the number of users further increases to  $K = 8$ , it is observed that the system with the proposed over-the-air beamforming-based scheme outperforms the system with the traditional ZF technique with a significant performance gain.

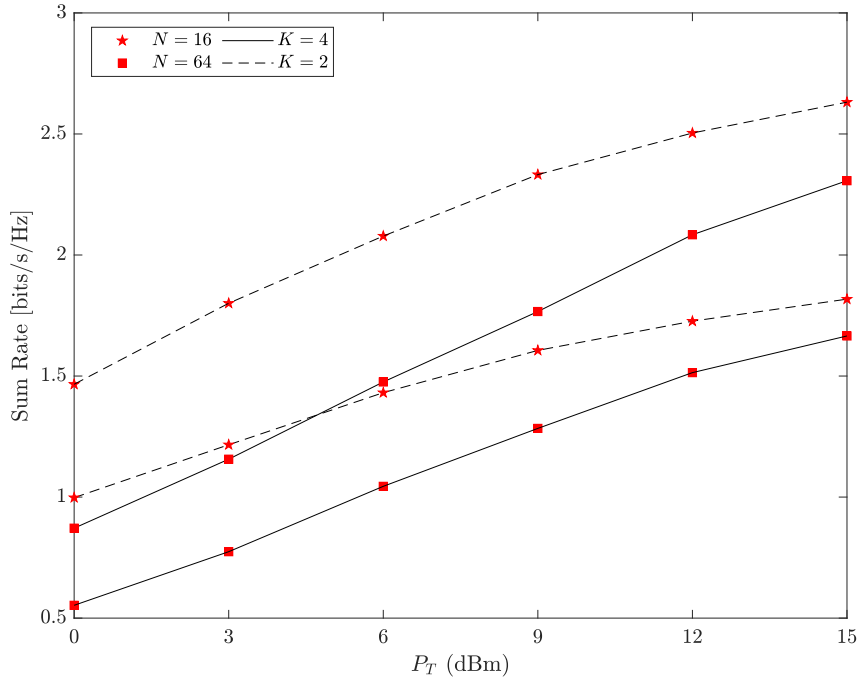


**Figure 4.** Sum-rate performance of the proposed over-the-air beamforming-based multi-user systems for different system configurations

In Figure 4, the sum-rate of the proposed over-the-air beamforming-based downlink multi-user system is evaluated for different system configurations. In this case, for a constant  $P_T$ , the performance of the over-the-air beamforming based systems are investigated for different number of the reflecting elements  $N$ ,  $P_{BS} = 0$  dBm and QPSK signaling. It is observed that increasing RIS size has an adverse affect on the system performance. This results may be explained by the fact that in the over-the-air beamforming design, as given in (11), the power consumed by the reflecting elements is inversely proportional with the magnitude of the channel matrix  $\mathbf{H}$ . Therefore, when a constant  $P_A$  is considered for  $N = 16$  and  $N = 64$ , it reveals that the proposed beamforming-based systems with the lower  $N$  values show considerably better performance than the ones with the higher  $N$  values.

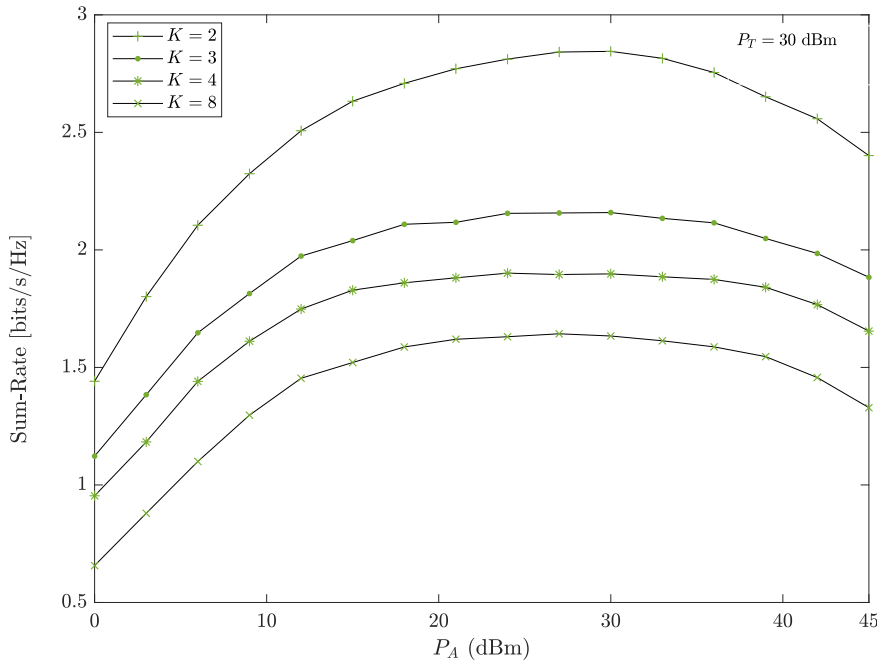


**Figure 5.** Sum-rate of the proposed over-the-air beamforming-based systems for  $N = 16$  and  $K \in \{2, 3, 4, 8\}$ .

In Figure 5, the effect of increasing reflection power  $P_A$  on the sum-rate of the proposed beamforming based systems with QPSK and  $P_T = 30$  dBm is investigated for  $N = 16$ . The results show that in all cases, the increasing  $P_A$  improves the system performance up to a certain  $P_A$  value, after which the performance begins to degrade. These results indicate the relation between the reflection power constraint  $P_A$  and transmitter power  $P_{BS}$  in (10). Indeed, in our system design, the overall consumed power  $P_T$  is dissipated to the transmitter ( $P_{BS}$ ) and the RIS ( $P_A$ ), where  $P_T = P_{BS} + P_A$ , and for a constant  $P_T = 30$  dBm,  $P_{BS}$  decreases with increasing  $P_A$ . However, it is clear from (6) that the minimizing  $P_{BS}$  directly affects the SINR value. Surely, the investigation of this interesting trade-off points out the importance of the power allocation between the transmitter and the RIS, which is an open problem to be addressed in future studies.

## 4.2 Single-user uplink transmission

In this subsection, the BER performance of the proposed receive IM scheme is evaluated.

In Figure 6, the BER performance of the proposed receive IM scheme with sub-optimal greedy detector is investigated for different RIS-aided MIMO configurations with  $N = 16$  and binary PSK (BPSK). Similar to the conventional receive IM schemes (Wu et al., 2021; Zhang et al., 2013), the performance results of the corresponding high-rate systems that employ (a)  $T_x = 2$  and (b)  $T_x = 4$  transmit antennas reveal a certain trade-off between system performance and data-rate.

In Figure 7, the BER performance of the transmit ZF precoded receive spatial modulation (RSM) (Zhang et al., 2013) and the proposed over-the-air receive IM schemes are compared. For  $R_x = T_x = 2$ , the receive IM and the RSM schemes respectively exploit BPSK and QPSK modulations to achieve  $\eta_{IM} = 3$  bits/s/Hz. On the other hand, for  $R_x = T_x = 4$  configuration, the receive IM with BPSK and the RSM with 16-PSK assess  $\eta_{IM} = 6$  bits/s/Hz. The results demonstrate the significant performance improvement of the proposed receive IM scheme over the traditional ZF precoded RSM (Zhang et al., 2013).

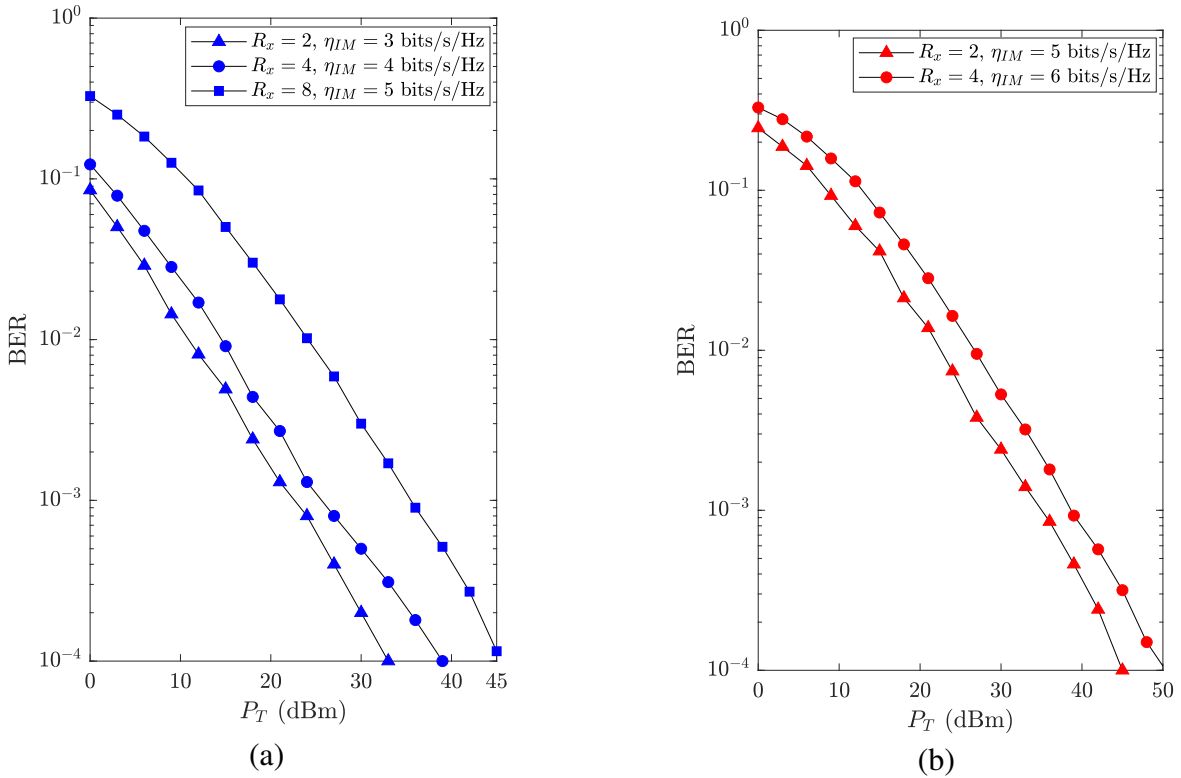


**Figure 6.** BER performance of the novel receive IM scheme with greedy detector for  $N = 16$  and (a)  $T_x = 2$ , (b)  $T_x = 4$

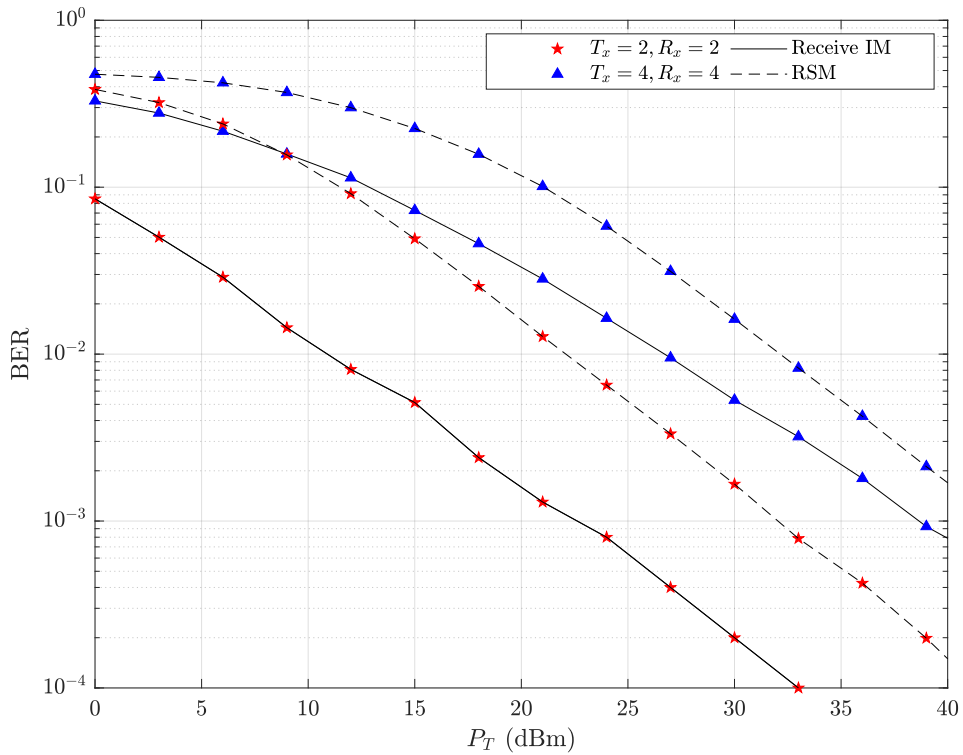


**Figure 7.** BER performance comparison of the proposed receive IM and RSM schemes.

## 5 CONCLUSION

In this paper, first, deploying an active RIS, a novel beamforming approach has been proposed for RIS-aided multi-user systems. In the proposed concept, without employing any other signal processing units at the transmitter and/or receiver sides, the reflection coefficients of the active RIS have been customized to mitigate the user interference. To meet this challenge, we have obtained SDR-based solutions via CVX software toolbox. Moreover, taking the proposed over-the-air beamforming concept one step further, a low-complexity receive IM scheme has been developed for single-user uplink transmission. Through computer simulations, the enhanced performance of the over-the-air beamforming-based systems over the traditional precoding-based systems have been indicated.

## CONFLICT OF INTEREST STATEMENT

The authors declare that the research was conducted in the absence of any commercial or financial relationships that could be construed as a potential conflict of interest.

## AUTHOR CONTRIBUTIONS

ZY, EB and IA contributed to the design and implementation of the research, to the analysis of the results and to the writing of the manuscript.

## FUNDING

This work was supported by the Scientific and Technological Research Council of Turkey (TUBITAK)-COST project 120E401.

## REFERENCES

- Almohamad, A., Tahir, A. M., Al-Kababji, A., Furqan, H. M., Khattab, T., Hasna, M. O., et al. (2020). Smart and secure wireless communications via reflecting intelligent surfaces: A short survey. *IEEE Open Journal of the Communications Society* 1, 1442–1456. doi:10.1109/OJCOMS.2020.3023731
- Basar, E. (2019). Transmission through large intelligent surfaces: A new frontier in wireless communications. In *2019 European Conference on Networks and Communications (EuCNC)* (IEEE), 112–117
- Basar, E. (2020). Reconfigurable intelligent surface-based index modulation: A new beyond MIMO paradigm for 6G. *IEEE Transactions on Communications* 68, 3187–3196. doi:10.1109/TCOMM.2020.2971486
- Basar, E., Di Renzo, M., De Rosny, J., Debbah, M., Alouini, M.-S., and Zhang, R. (2019). Wireless communications through reconfigurable intelligent surfaces. *IEEE Access* 7, 116753–116773
- Basar, E. and Poor, H. V. (2021). Present and future of reconfigurable intelligent surface-empowered communications [perspectives]. *IEEE Signal Processing Magazine* 38, 146–152. doi:10.1109/MSP.2021.3106230
- Basar, E., Wen, M., Mesleh, R., Di Renzo, M., Xiao, Y., and Haas, H. (2017). Index modulation techniques for next-generation wireless networks. *IEEE Access* 5, 16693–16746. doi:10.1109/ACCESS.2017.2737528

- Basar, E., Yildirim, I., and Kilinc, F. (2021). Indoor and outdoor physical channel modeling and efficient positioning for reconfigurable intelligent surfaces in mmWave bands. *IEEE Transactions on Communications* 69, 8600–8611. doi:10.1109/TCOMM.2021.3113954
- Björnson, E., Özdogan, Ö., and Larsson, E. G. (2019). Intelligent reflecting surface versus decode-and-forward: How large surfaces are needed to beat relaying? *IEEE Wireless Communications Letters* 9, 244–248. doi:10.1109/LWC.2019.2950624
- Dai, L., Wang, B., Wang, M., Yang, X., Tan, J., Bi, S., et al. (2020). Reconfigurable intelligent surface-based wireless communications: Antenna design, prototyping, and experimental results. *IEEE Access* 8, 45913–45923. doi:10.1109/ACCESS.2020.2977772
- Di, B., Zhang, H., Song, L., Li, Y., Han, Z., and Poor, H. V. (2020). Hybrid beamforming for reconfigurable intelligent surface based multi-user communications: Achievable rates with limited discrete phase shifts. *IEEE Journal on Selected Areas in Communications* 38, 1809–1822. doi:10.1109/JSAC.2020.3000813
- Di Renzo, M., Zappone, A., Debbah, M., Alouini, M.-S., Yuen, C., De Rosny, J., et al. (2020). Smart radio environments empowered by reconfigurable intelligent surfaces: How it works, state of research, and the road ahead. *IEEE Journal on Selected Areas in Communications* 38, 2450–2525. doi:10.1109/JSAC.2020.3007211
- Dong, L. and Wang, H.-M. (2020). Secure MIMO transmission via intelligent reflecting surface. *IEEE Wireless Communications Letters* 9, 787–790. doi:10.1109/LWC.2020.2969664
- El Ayach, O., Rajagopal, S., Abu-Surra, S., Pi, Z., and Heath, R. W. (2014). Spatially sparse precoding in millimeter wave mimo systems. *IEEE Transactions on Wireless Communications* 13, 1499–1513. doi:10.1109/TWC.2014.011714.130846
- Ferreira, R. C., Facina, M. S., De Figueiredo, F. A., Fraidenraich, G., and De Lima, E. R. (2020). Bit error probability for large intelligent surfaces under double-Nakagami fading channels. *IEEE Open Journal of the Communications Society* 1, 750–759. doi:10.1109/OJCOMS.2020.2996797
- Gao, Y., Wu, Q., Zhang, G., Chen, W., Ng, D. W. K., and Di Renzo, M. (2022). Beamforming optimization for active intelligent reflecting surface-aided SWIPT. *arXiv preprint arXiv:2203.16093*
- Gong, S., Lu, X., Hoang, D. T., Niyato, D., Shu, L., Kim, D. I., et al. (2020). Toward smart wireless communications via intelligent reflecting surfaces: A contemporary survey. *IEEE Communications Surveys & Tutorials* 22, 2283–2314. doi:10.1109/COMST.2020.3004197
- Grant, M. and Boyd, S. (2008). Graph implementations for nonsmooth convex programs. In *Recent Advances in Learning and Control*, eds. V. Blondel, S. Boyd, and H. Kimura (Springer-Verlag Limited), Lecture Notes in Control and Information Sciences. 95–110. [http://stanford.edu/~boyd/graph\\_dcp.html](http://stanford.edu/~boyd/graph_dcp.html)
- Guo, S., Lv, S., Zhang, H., Ye, J., and Zhang, P. (2020). Reflecting modulation. *IEEE Journal on Selected Areas in Communications* 38, 2548–2561. doi:10.1109/JSAC.2020.3007060
- Huang, C., Zappone, A., Alexandropoulos, G. C., Debbah, M., and Yuen, C. (2019). Reconfigurable intelligent surfaces for energy efficiency in wireless communication. *IEEE Transactions on Wireless Communications* 18, 4157–4170. doi:10.1109/TWC.2019.2922609
- Kilinc, F., Yildirim, I., and Basar, E. (2021). Physical channel modeling for RIS-empowered wireless networks in sub-6 GHz bands. In *2021 55th Asilomar Conference on Signals, Systems, and Computers (IEEE)*, 704–708
- Kundu, N. K. and McKay, M. R. (2021). Channel estimation for reconfigurable intelligent surface aided MISO communications: From LMMSE to deep learning solutions. *IEEE Open Journal of the Communications Society* 2, 471–487. doi:10.1109/OJCOMS.2021.3063171

- Li, Q., Wen, M., and Di Renzo, M. (2021). Single-RF MIMO: From spatial modulation to metasurface-based modulation. *IEEE Wireless Communications* 28, 88–95. doi:10.1109/MWC.021.2000376
- Lin, S., Zheng, B., Alexandropoulos, G. C., Wen, M., Di Renzo, M., and Chen, F. (2020). Reconfigurable intelligent surfaces with reflection pattern modulation: Beamforming design and performance analysis. *IEEE Transactions on Wireless Communications* 20, 741–754. doi:10.1109/TWC.2020.3028198
- Long, R., Liang, Y.-C., Pei, Y., and Larsson, E. G. (2021). Active reconfigurable intelligent surface-aided wireless communications. *IEEE Transactions on Wireless Communications* 20, 4962–4975. doi:10.1109/TWC.2021.3064024
- Luo, S., Yang, P., Che, Y., Yang, K., Wu, K., Teh, K. C., et al. (2021). Spatial modulation for RIS-assisted uplink communication: Joint power allocation and passive beamforming design. *IEEE Transactions on Communications* 69, 7017–7031. doi:10.1109/TCOMM.2021.3096965
- Luo, Z.-Q., Ma, W.-K., So, A. M.-C., Ye, Y., and Zhang, S. (2010). Semidefinite relaxation of quadratic optimization problems. *IEEE Signal Processing Magazine* 27, 20–34. doi:10.1109/MSP.2010.936019
- Nguyen, N. T., Vu, D., Lee, K., and Juntti, M. (2022). Hybrid relay-reflecting intelligent surface-assisted wireless communications. *IEEE Transactions on Vehicular Technology* doi:10.1109/TVT.2022.3158686
- Perović, N. S., Tran, L.-N., Di Renzo, M., and Flanagan, M. F. (2021). Achievable rate optimization for MIMO systems with reconfigurable intelligent surfaces. *IEEE Transactions on Wireless Communications* 20, 3865–3882. doi:10.1109/TWC.2021.3054121
- Sohrabi, F. and Yu, W. (2016). Hybrid digital and analog beamforming design for large-scale antenna arrays. *IEEE Journal of Selected Topics in Signal Processing* 10, 501–513. doi:10.1109/JSTSP.2016.2520912
- Spencer, Q. H., Swindlehurst, A. L., and Haardt, M. (2004). Zero-forcing methods for downlink spatial multiplexing in multiuser MIMO channels. *IEEE Transactions on Signal Processing* 52, 461–471. doi:10.1109/TSP.2003.821107
- Stavridis, A., Sinanovic, S., Di Renzo, M., and Haas, H. (2012). Transmit precoding for receive spatial modulation using imperfect channel knowledge. In *2012 IEEE 75th Vehicular Technology Conference (VTC Spring)* (IEEE), 1–5
- Taha, A., Alrabeiah, M., and Alkhateeb, A. (2021). Enabling large intelligent surfaces with compressive sensing and deep learning. *IEEE Access* 9, 44304–44321. doi:10.1109/ACCESS.2021.3064073
- Tang, W., Dai, J. Y., Chen, M. Z., Wong, K.-K., Li, X., Zhao, X., et al. (2020). MIMO transmission through reconfigurable intelligent surface: System design, analysis, and implementation. *IEEE journal on selected areas in communications* 38, 2683–2699. doi:10.1109/JSAC.2020.3007055
- Thanh Nguyen, N., Nguyen, V.-D., Wu, Q., Tolli, A., Chatzinotas, S., and Juntti, M. (2022). Hybrid active-passive reconfigurable intelligent surface-assisted multi-user MISO systems. *arXiv e-prints*, arXiv–2203
- Wu, M., Lei, X., Zhou, X., Xiao, Y., Tang, X., and Hu, R. Q. (2021). Reconfigurable intelligent surface assisted spatial modulation for symbiotic radio. *IEEE Transactions on Vehicular Technology* 70, 12918–12931. doi:10.1109/TVT.2021.3121698
- Wu, Q. and Zhang, R. (2019). Intelligent reflecting surface enhanced wireless network via joint active and passive beamforming. *IEEE Transactions on Wireless Communications* 18, 5394–5409. doi:10.1109/TWC.2019.2936025
- Yan, W., Yuan, X., He, Z.-Q., and Kuai, X. (2020). Passive beamforming and information transfer design for reconfigurable intelligent surfaces aided multiuser mimo systems. *IEEE Journal on Selected Areas in Communications* 38, 1793–1808. doi:10.1109/JSAC.2020.3000811



- Ye, J., Guo, S., and Alouini, M.-S. (2020). Joint reflecting and precoding designs for SER minimization in reconfigurable intelligent surfaces assisted MIMO systems. *IEEE Transactions on Wireless Communications* 19, 5561–5574. doi:10.1109/TWC.2020.2994455
- Yigit, Z., Basar, E., and Altunbas, I. (2020). Low complexity adaptation for reconfigurable intelligent surface-based MIMO systems. *IEEE Communications Letters* 24, 2946–2950. doi:10.1109/LCOMM.2020.3014820
- Yigit, Z., Basar, E., and Altunbas, I. (2021a). SimMBM channel simulator for media-based modulation systems. In *2021 IEEE 32nd Annual International Symposium on Personal, Indoor and Mobile Radio Communications (PIMRC) (IEEE)*, 531–536
- Yigit, Z., Basar, E., Wen, M., and Altunbas, I. (2021b). Hybrid reflection modulation. *arXiv preprint arXiv:2111.08355*
- Yu, X., Xu, D., and Schober, R. (2019). MISO wireless communication systems via intelligent reflecting surfaces. In *2019 IEEE/CIC International Conference on Communications in China (ICCC) (IEEE)*, 735–740
- Zhang, J., Zhang, Y., Zhong, C., and Zhang, Z. (2020). Robust design for intelligent reflecting surfaces assisted MISO systems. *IEEE Communications Letters* 24, 2353–2357. doi:10.1109/LCOMM.2020.3002557
- Zhang, R., Yang, L.-L., and Hanzo, L. (2013). Generalised pre-coding aided spatial modulation. *IEEE Transactions on Wireless Communications* 12, 5434–5443. doi:10.1109/TWC.2013.100213.130848
- Zhang, S. and Zhang, R. (2020). Capacity characterization for intelligent reflecting surface aided MIMO communication. *IEEE Journal on Selected Areas in Communications* 38, 1823–1838. doi:10.1109/JSAC.2020.3000814
- Zhang, X. (2017). *Matrix analysis and applications* (Cambridge University Press)
- Zhang, Z., Dai, L., Chen, X., Liu, C., Yang, F., Schober, R., et al. (2021). Active RIS vs. passive RIS: Which will prevail in 6G? *arXiv preprint arXiv:2103.15154*